



Multi-model assessment of impacts of the 2022 Hunga eruption on stratospheric ozone and its chemical and dynamical drivers

Ewa M. Bednarz^{1,2}, Valentina Aquila³, Amy H. Butler², Peter Colarco^{4,5}, Eric Fleming^{4,6}, Freja F. Østerstrøm^{7,8}, David Plummer⁹, Ilaria Quaglia¹⁰, William Randel¹⁰, Michelle L. Santee¹¹, Takashi Sekiya¹², Simone Tilmes¹⁰, Xinyue Wang¹³, Shingo Watanabe^{12,14}, Wandi Yu¹⁵, Jun Zhang¹⁰, Yunqian Zhu^{1,2}, Zhihong Zhuo¹⁶

- 1. Cooperative Institute for Research in Environmental Sciences (CIRES), University of Colorado Boulder, Boulder, CO, USA.
- 10 2. NOAA Chemical Sciences Laboratory (NOAA CSL), Boulder, CO, USA
 - 3. American University, Department of Environmental Science, Washington, DC, USA
 - 4. NASA Goddard Space Flight Center, Greenbelt, MD, USA
 - 5. Earth System Science Interdisciplinary Center, University of Maryland, College Park, MD, USA
 - 6. Science Systems and Applications, Inc., Lanham, MD, USA
- 7. Department of Environmental Science, Aarhus University, Roskilde, Denmark.
 - 8. School of Engineering and Applied Sciences, Harvard University, Cambridge, MA, USA.
 - 9. Climate Research Division, Environment and Climate Change Canada, Montréal, Canada
 - 10. NSF National Center for Atmospheric Research, Boulder, CO, USA
 - 11. Jet Propulsion Laboratory, California Institute of Technology, Pasadena, CA, USA.
- 20 12. Japan Agency for Marine-Earth Science and Technology (JAMSTEC), Yokohama, Japan
 - 13. Department of Atmospheric and Oceanic Sciences, University of Colorado Boulder, Boulder, CO, USA
 - 14. Advanced Institute for Marine Ecosystem Change (WPI-AIMEC), Tohoku University, Sendai, Japan
 - 15. Lawrence Livermore National Laboratory, CA, USA
 - 16. Department of Earth and Atmospheric Sciences, University of Quebec in Montreal, Montreal (Quebec), Canada.

Correspondence to: Ewa M. Bednarz (ewa.bednarz@noaa.gov)

Abstract.

25

The 2022 Hunga eruption injected unprecedented quantities of water vapor into the stratosphere, alongside modest amounts of aerosol precursors. There remain uncertainties regarding the extent to which it influenced the stratospheric ozone layer.

We address this using a multi-model ensemble of chemistry-climate model simulations, assessing the impacts of Hunga-induced perturbations in both water vapor and aerosol by combining free-running and specified-dynamics experiments. The results confirm that the Hunga eruption contributed to the anomalously low ozone abundances observed in the southern mid-latitudes in 2022. The simulations also indicate enhanced ozone depletion inside the Antarctic polar vortex, albeit with significant differences in magnitude and persistence across the models. Our results indicate that the chemical contribution was as important as the dynamical contribution in determining the overall ozone response to the Hunga eruption in the southern extra-tropics, with anomalous chemical (chlorine, bromine and nitrogen) processing on aerosol surfaces under





conditions of water-induced stratospheric cooling together with dynamical contributions from altered circulation and ozone transport. Finally, while Hunga may continue to exert a smaller influence on ozone as the anomalous water vapor and aerosol is removed from the atmosphere, natural dynamical variability will likely hinder detection of any such influences, with the most robust Hunga signal expected in the upper stratosphere. Our study confirms the eruption's role in modulating stratospheric ozone levels in the short term, but also highlights the associated uncertainties and the presence of large natural variability, all of which makes confident attribution of the Hunga impacts an ongoing challenge.

1. Introduction

45

55

The 15 January 2022 eruption of the Hunga volcano injected water vapor and other volcanic material into the stratosphere and lower mesosphere (Proud et al., 2022; Carr et al., 2022). Aura Microwave Limb Sounder (MLS) remote sensing measurements suggest that the eruption increased the global stratospheric water vapor burden by approximately 10-15% (Khaykin et al., 2022; Vömel et al., 2022), equivalent to ~ 150 Tg of water vapor (Millán et al., 2022), making it the largest stratospheric water vapor perturbation in the satellite era. The radiative cooling by the anomalous water vapor led to upper stratospheric cooling of up to a few degrees K that was observed in 2022 and 2023 (Coy et al., 2022; Stocker, et al., 2024; Wang et al. 2023; Randel et al., 2024; Schoeberl et al., 2023; 2024; Stenchikov et al., 2025, Zhuo et al., 2025). The eruption also injected moderate amounts (~0.5-1.0 Tg) of SO₂ (Millán et al., 2022, Carn et al., 2023; Sellitto et al., 2024), which converted quickly to form stratospheric aerosols (Asher et al., 2023).

Given the presence of stratospheric aerosols alongside anomalous water vapor and the associated perturbations in stratospheric temperatures, a question emerged whether the eruption could also have a significant impact on the ozone layer. In the upper stratosphere and lower mesosphere, both MLS observations and chemistry-climate models show ozone reductions of a few percent from late 2022 onwards due to enhanced hydrogen oxide (HOx) catalyzed chemical loss in the presence of anomalous water vapor (Randel et al., 2024; Zhuo et al., 2025). At lower altitudes, however, the impact of the eruption remains less clear. MLS observations showed exceptionally low ozone abundances in the Southern Hemisphere (SH) mid-latitude lower stratosphere, alongside some significant perturbation to other chemical tracers, in mid-to-late 2022, and tracer-tracer correlation analysis suggested that this ozone reduction was largely controlled by transport (Santee et al, 2023). Follow-on studies combining numerical model simulations with observations examined the origin of these anomalies more deeply. While Wilmouth et al (2023) reported that both chemical and dynamical changes were important in driving those changes, Zhang et al. (2024a) indicated that the anomalous chemical processing under Hunga aerosol and water vapor, whilst significant, was secondary in importance, and that anomalous dynamical variability was likely the dominant driver of the anomalies observed in the SH mid-latitudes in 2022. Such exceptional dynamical variability could be a manifestation of large natural variability of the extra-tropical stratosphere, but it could also be partly driven by the Hunga impact on atmospheric circulation and transport. Indeed, using Community Earth System Model (CESM) simulations Wang et al.



70

75

80

90

95

100



(2023) showed that the Hunga forcing likely led to a strengthening and equatorward shift of the SH stratospheric jet in austral winter of 2022. The simulated response was qualitatively similar to that seen in reanalysis data and was associated with weakening of the large-scale residual circulation and ozone transport, thus likely contributing to the ozone reductions observed in the SH mid-latitudes. However, the model circulation response was still much weaker than that in the reanalysis, suggesting that the dynamical response to the Hunga forcing could only explain part of the observed anomaly and that the observational record contains significant natural variability unrelated to the Hunga forcing. Hence, the extent to which Hunga forcing contributed to the anomalously low SH mid-latitude ozone abundances remains unclear.

For Antarctic ozone, little impact was observed in the satellite record in 2022 as the Hunga water vapor was excluded from the polar vortex (Manney et. al., 2023), and uncertainties remain whether or not the same was the case for Hunga aerosol. In 2023, CALIOP (Cloud-Aerosol Lidar with Orthogonal Polarization) space-based lidar and MLS observations indicated exceptional polar stratospheric cloud (PSC) formation and chlorine activation earlier in austral winter and at higher altitudes than average, likely due to the extra water vapor, but the PSC activity was followed by significant dehydration through PSC sedimentation. As a result, Antarctic ozone levels observed in spring 2023 were within the (relatively large) range of interannual variability (Santee et al., 2024). Since isolation of the Hunga impact based solely on the observational record is intrinsically challenging, model simulations were carried out under a setup that allows isolation of the Hunga effects more clearly, and these have yielded contrasting results. Using a 2D model forced with the anomalous water vapor from Hunga, Fleming et al. (2024) reported additional total column ozone losses from the eruption of up to ~25 DU in late 2023 over the SH pole (with the value dependent on the background meteorological conditions assumed), persisting with decreasing magnitude for the following few years as Hunga water is gradually removed from the atmosphere. Using a chemistry transport model (CTM) also forced with just Hunga water vapor, Zhou et al (2024) showed smaller but still significant ozone losses of up to 10 DU in late 2023 in the collar region around the vortex edge. In contrast, Wohltmann at al. (2024) used a combination of both a CTM and MLS data and estimated only a minor (< 4 DU) additional ozone loss from the chemical impacts of the water vapor (compared to ~110 DU and ~140 DU total chemical loss in the vortex averaged stratospheric partial ozone column estimated from the CTM and MLS data, respectively). Importantly, none of these models included injection of aerosols (or SO₂) by the eruption, nor could they simulate the full impacts on atmospheric circulation. Hence, considerable uncertainty remains regarding impacts of the eruption on both past and future ozone.

Here we address this uncertainty in Hunga ozone impacts using a multi-model ensemble of chemistry-climate model simulations performed as part of the Hunga Tonga-Hunga Ha'apai Volcano Impact Model Observation Comparison (HTHH-MOC) project (Zhu et al., 2025). The models simulated the impacts of both Hunga water and aerosol perturbations, both together and separately, and were run using free-running and specified dynamics (i.e. with meteorology 'nudged' to reanalysis data) configurations. The use of such experiments, and in a multi-model framework, allows us to not only assess



115

120

125

130



the impact of the eruption on ozone but also examine the relative importance of the Hunga forcing on its different chemical and dynamical drivers.

2. Model simulations

We use the model simulations performed for the HTHH-MOC project (Zhu et al., 2025). We leverage the results of four chemistry-climate models: the NASA Goddard Earth Observing System Chemistry-Climate Model (GEOSCCM; Reinecker et al., 2008; Molod et al., 2015), the Model for Interdisciplinary Research On Climate – CHemical Atmospheric general circulation model for Study of atmospheric Environment and Radiative forcing version 6 (MIROC-CHASER; Sekiya et al., 2016), the Whole Atmosphere Community Climate Model version 6 coupled to the Modal Aerosol Microphysics module version 4 (WACCM-MAM; Gettelman et al., 2019), and the Canadian Middle Atmosphere Model (CMAM; Scinocca et al., 2008). We also use results from one simplified 2D model: the NASA/Goddard Space Flight Center two-dimensional chemistry-climate model (GSFC2D; Fleming et al., 2024).

First, we focus on the results from GEOSCCM, MIROC-CHASER and WACCM-MAM, all of which performed a set of both free-running ('FREE') and specified-dynamics (nudged, 'NDGD') experiments, each consisting of simulations with the Hunga forcing included (injection of one or both of 0.5 Tg SO₂ and ~150 Tg H₂O) and control simulations without Hunga injection. For each experiment, the response is taken as the difference between the perturbed and the control simulations. Note that models injected the volcanic material at slightly different altitudes in the stratosphere, and for H₂O the ~150 Tg is not an actual injection magnitude, but rather the amount left after a week. The free-running experiments span 10 years (2022-2031) and include simultaneous injection of both SO₂ and H₂O as well as imposed climatological sea-surface temperatures and sea-ice (same in both control and perturbed experiments). GEOSCCM and MIROC-CHASER performed ensemble simulations consisting of 10 ensemble members for each of the perturbed and control experiments, and WACCM-MAM simulations include 30 ensemble members each; in each case only the ensemble mean response is analyzed. The nudged simulations, injecting SO₂ and H₂O, SO₂-only or H₂O-only, span 2022-2023 and are forced with observed seasurface temperatures and sea-ice and constrained meteorology, with atmospheric temperatures and winds nudged to those given by the Modern-Era Retrospective analysis for Research and Applications version 2 reanalysis (MERRA-2, Gelaro et al., 2017; same for both the perturbed and control simulations). Finally, we compare the results with those of free-running simulations in which only H₂O was injected; this experiment has been performed by MIROC-CHASER, CMAM and GSFC2D (the latter is also discussed by Fleming et al., 2024), with 10 ensemble members each. The summary of model simulations used is given in Table 1; a detailed description of the experimental setup and individual models can be found in Zhu et al. (2025; where our FREE simulations are denoted 'Exp1 FixedSST', and our NDGD simulations are denoted 'Exp2').



140

145



Figure 1 shows the evolution of the anomalous aerosol surface area density (SAD) and water vapor simulated in the SH extra-tropics (90°S-30°S) by the three models that performed the free-running experiment with simultaneous injection of SO₂ and H₂O. The response is taken to be statistically significant if it exceeds ± 2 standard errors in the difference in means (i. e. $\sqrt{\frac{\sigma_1^2}{n_1} + \frac{\sigma_2^2}{n_2}}$, where σ denotes standard deviation and $n_1 = n_2 = 30$ denotes the sample size of each of the perturbed and control distributions). As also discussed by Zhuo et al. (2025), while models show overall similar evolution of the anomalous aerosol and water vapor from the eruption, they also show notable differences. For aerosols, while GEOSCCM and WACCM-MAM simulate substantial enhancements of aerosol SAD persisting in the lower stratosphere until at least the end of 2025, in MIROC-CHASER the magnitude of the SAD perturbation is much larger and persists for longer. For water vapor, all three models simulate the largest concentrations confined to the middle stratosphere in 2022, followed by upward transport within the ascending branch of the Brewer-Dobson circulation in 2023. As a result, the upper stratospheric water vapor anomalies peak in late 2023 and decline afterwards, although with notably different lifetimes across the models (Zhuo et al., 2025). Overall similar aerosol and water vapor anomalies were simulated in the corresponding nudged simulations (Figure S1 and S2), although some differences arise because of the differences in the simulated transport between the free-running and the nudged setups as well as non-additivity of the single-forcing perturbations, even under constrained meteorology.

	Free-running (FREE)		Nudged (NDGD)		
	SO ₂ +H ₂ O	H ₂ O-only	SO ₂ +H ₂ O	SO ₂ -only	H ₂ O-only
GEOSCCM	X		X	X	Х
MIROC-	Х	Х	X	X	Х
CHASER	Α	Α	Λ	Λ	Λ
WACCM-MAM	Х		X	X	Х
CMAM		X			
GSFC2D		X			X

Table 1. Summary of model simulations used in this study.





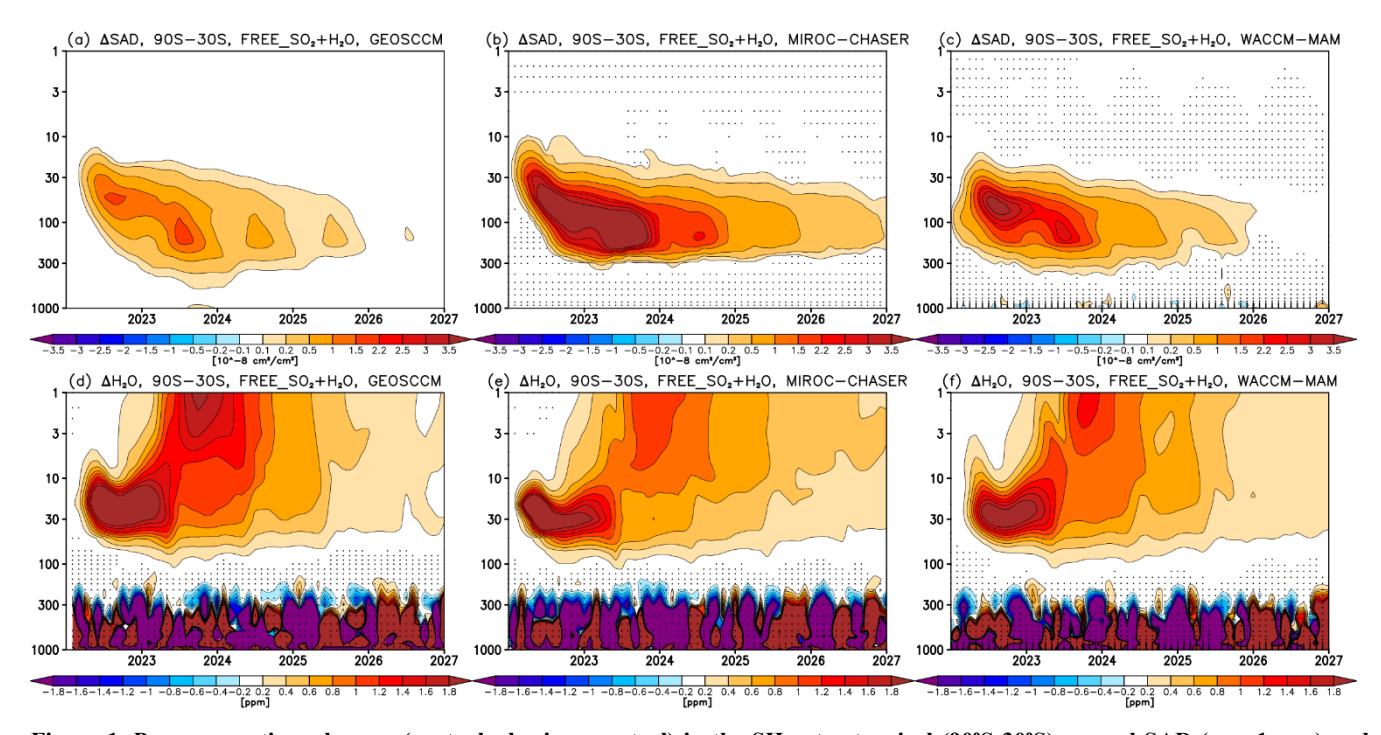


Figure 1. Pressure vs time changes (perturbed minus control) in the SH extra-tropical (90°S-30°S) aerosol SAD (row 1; a-c) and water vapor (row 2; d-f) simulated in the free-running experiment with simultaneous injection of SO₂ and H₂O (FREE_SO₂+H₂O) in GEOSCCM (left; a,d), MIROC-CHASER (middle; b,e) and WACCM-MAM (right; c,f). Stippling marks regions where the response is not statistically significant (with the response taken to be significant if it exceeds ±2 standard errors in the difference in means). See Fig. S1 and S2 (in the supplementary material) for the changes simulated in the nudged experiments.

3. Results

160

165

3.1. Simulated ozone responses

Figure 2 shows simulated changes (perturbed Hunga simulations minus control simulations) in total column ozone simulated by the three chemistry-climate models (GEOSCCM, MIROC-CHASER and WACCM-MAM) in the different free-running and nudged experiments. In the free-running simulations (row 1; a-c), which inject both SO₂ and H₂O and include Hunga impacts on all the different chemical, radiative and dynamical processes, all three models simulate total column ozone decreases in the SH mid-latitudes and springtime high latitudes following the eruption, although with large differences in the magnitudes and duration of the effects. GEOSCCM shows the largest Antarctic ozone reductions (of up to ~50 DU in late 2023), with statistically significant total column ozone reductions in the SH mid- and high latitudes persisting until 2026. MIROC-CHASER shows the smallest response, with ozone losses of a few DU in the SH mid-latitudes from late 2022 into early 2024, and statistically not significant ozone losses in the Antarctic in late 2022 and 2023. While WACCM-MAM also shows ozone losses of a few DU in the SH mid-latitudes from mid-2022 into early 2024, it simulates considerably larger ozone reductions in the Antarctic (of up to ~15 DU and ~20 DU in the zonal mean in late 2022 and 2023, respectively).



185

190

195

200



Row 2 in Fig. 2 shows the corresponding responses to SO₂+H₂O injections in the nudged experiments; by design, these include only direct chemical impacts of the eruption on ozone and not any impacts driven by changes in temperatures or circulation (because the meteorology is identical for the Hunga and control simulations, and so any forced response in it cancels out). Comparison of the free-running and nudged responses (i.e., row 1 vs row 2 in Fig. 2) shows that a significant part of the total response (Fig 2, row 1) is evident in the nudged simulations. Taking the Antarctic response in late 2023 as an example, GEOSCCM shows ozone loss of up to ~50 DU in the free-running experiment and ~25 DU in the nudged one, while for WACCM-MAM these ozone losses are ~20 DU and ~10 DU, respectively. This indicates that the Hunga impact on SH extra-tropical ozone, at least as simulated by these three models, is driven by a combination of both chemical and dynamical/temperature changes, the contributions of each roughly comparable in importance. Furthermore, isolating the contributions of SO₂-only and H₂O-only injections in the nudged simulations (rows 3 and 4) shows that the total column response due to chemistry is driven primarily by the aerosol forcing, with the H₂O forcing in isolation inducing only small total column ozone losses (up to ~5 DU), although the two forcings are not strictly additive (as will be discussed below).

As most of the ozone depletion from Hunga is found in the SH extra-tropics, Fig. 3 shows the vertical distribution of the 90°S-30°S mean ozone anomalies. The free-running simulations (row 1) show a distinct pattern of ozone anomalies that is consistent across all three models, with ozone decreasing in the upper stratosphere, increasing in the middle stratosphere (near ~30-10 hPa), and decreasing again in the lower stratosphere. Comparison with the corresponding nudged response (row 2) shows that, as noted earlier, a significant portion of the total response (row 1) is found in the nudged simulations, indicating that Hunga impacts on both chemical and dynamical/radiative processes are important in determining the overall ozone distribution following the eruption.

Notably, the lower stratospheric ozone reduction extends into the troposphere and affects ozone all the way to the surface, with ozone losses of a few percent in the SH extra-tropical free troposphere (500 hPa, Fig. 4, row 1) simulated by models until at least 2024. Stratospheric ozone tracer (O3S, e.g. Banerjee et al., 2016) is a proxy for the stratospheric origin of ozone in the troposphere; in the stratosphere O3S equals ozone concentrations, while in the troposphere it has no chemical production source (but it still undergoes chemical loss). Comparison of the tropospheric ozone response with the corresponding O3S response (row 2 in Fig. 4; note that the O3S tracer was not included in GEOSCCM) shows good qualitative and quantitative agreement, indicating the predominantly stratospheric origin of the negative tropospheric ozone anomalies via weakening of stratosphere-to-troposphere ozone transport. While O3S was not included in the GEOSCCM simulations, that model shows the largest tropospheric ozone losses (Fig. 4a) among all three models; these decreases are in agreement with the largest concurrent lower stratospheric ozone reductions (Fig. 3a), thus also pointing towards stratospheric origin of the tropospheric ozone anomalies.

In the following sections, we discuss the different chemical, dynamical and radiative drivers of the simulated Hunga ozone responses.





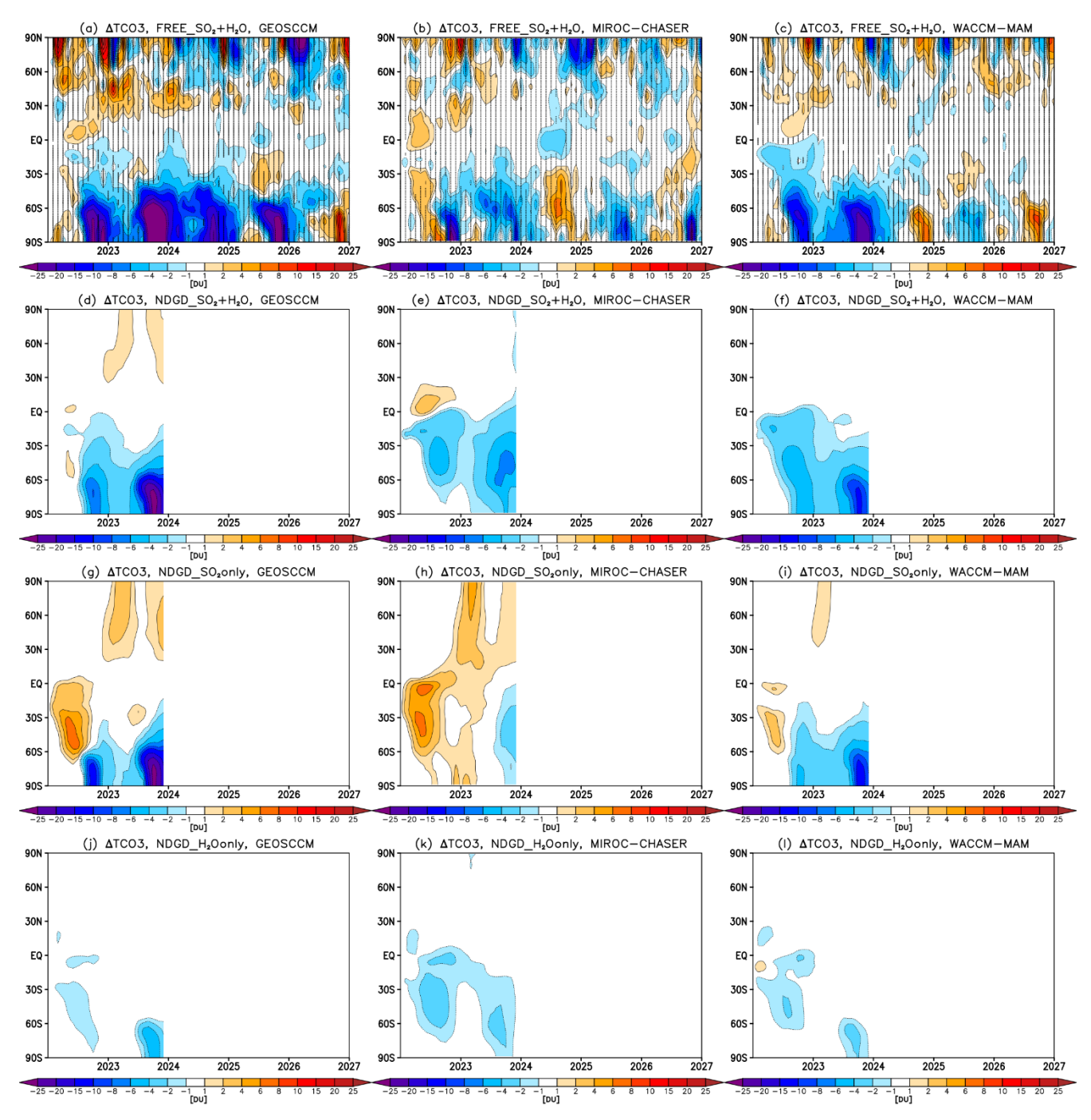


Figure 2. Latitude vs time changes (perturbed minus control) in total column ozone (TCO3) simulated in GEOSCCM (left; a,d,g,j), MIROC-CHASER (middle; b,e,h,k) and WACCM-MAM (right; c,f,i,l). Row 1 is for the free-running experiment with simultaneous injection of SO2 and H₂O (stippling defined as in Fig. 1). Rows 2-4 are for the nudged simulations (2022-2023), with SO2+H₂O injection (row 2), SO2-only injection (row 3) or H₂O-only injection (row 4).





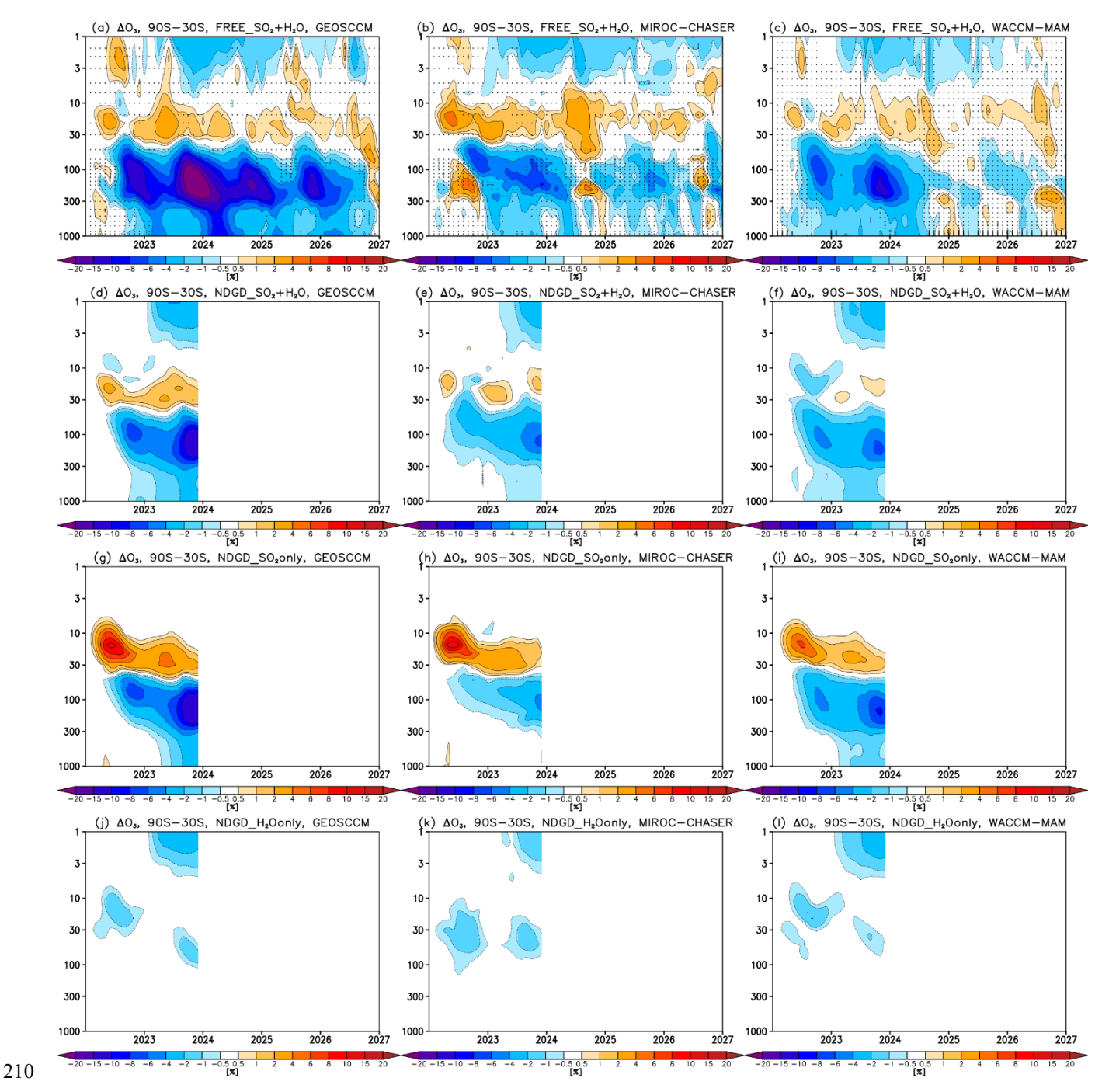


Figure 3. Pressure vs time changes in the SH extra-tropical (90°S-30°S) ozone mixing ratios simulated in GEOSCCM (left; a,d,g,j), MIROC-CHASER (middle; b,e,h,k) and WACCM-MAM (right; c,f,i,l). Row 1 is for the free-running experiment with simultaneous injection of SO₂ and H₂O (stippling defined as in Fig. 1). Rows 2-4 are for the nudged simulations (2022-2023), with SO₂+H₂O injection (row 2), SO₂-only injection (row 3) or H₂O-only injection (row 4).





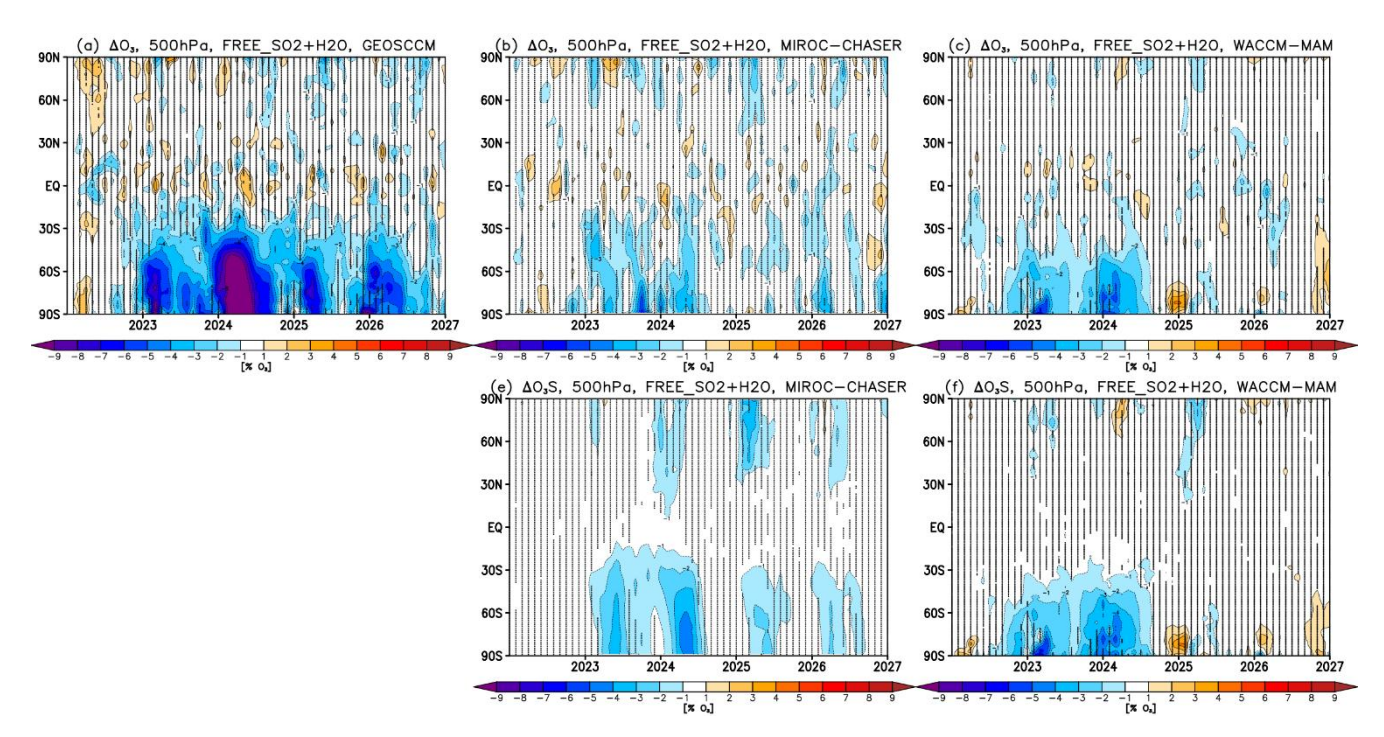


Figure 4. Latitude vs time changes (perturbed minus control) in 500 hPa ozone (row 1) and stratospheric ozone tracer O3S (row 2), with both expressed as % change with respect to the corresponding ozone values in the control experiment, simulated in the free-running experiment with simultaneous injection of SO₂ and H₂O in GEOSCCM (left; note the model did not include O3S tracer), MIROC-CHASER (middle) and WACCM-MAM (right). Stippling marks regions where the response is not statistically significant (defined as in Fig. 1). See Fig. S3 for the corresponding changes simulated in the nudged simulations.

3.2. Changes in chemical ozone drivers

225

230

In the upper stratosphere, the timescales of chemical processes are generally much faster than dynamical timescales, and so ozone concentrations are by and large in photochemical equilibrium. Accordingly, Fig. 3 shows that in the upper stratosphere the ozone response simulated in the nudged SO₂+H₂O experiment (Fig. 3, row 2) accounts for most of the full ozone response (Fig. 3, row 1), indicating that the Hunga impact in this region is largely chemically driven. In particular, the enhanced water vapor (Fig. 1 and S2) accelerates HOx-catalyzed ozone depletion (see also Santee et al., 2023; Wilmouth et al., 2023; Randel et al., 2024). The H₂O forcing from the eruption is the dominant driver of the ozone response in this region (Fig. 3, bottom row), with SO₂ injection having no discernable impact at these altitudes (Fig. 3, row 3). Consistent with this picture, the evolution of global-mean upper stratospheric ozone anomalies in these three models tracks closely the evolution of water vapor, with the models projecting that the Hunga water will continue to exert a small impact on upper stratospheric ozone until at least 2028 (Fig. 5; see also Zhuo et al. 2025).



255



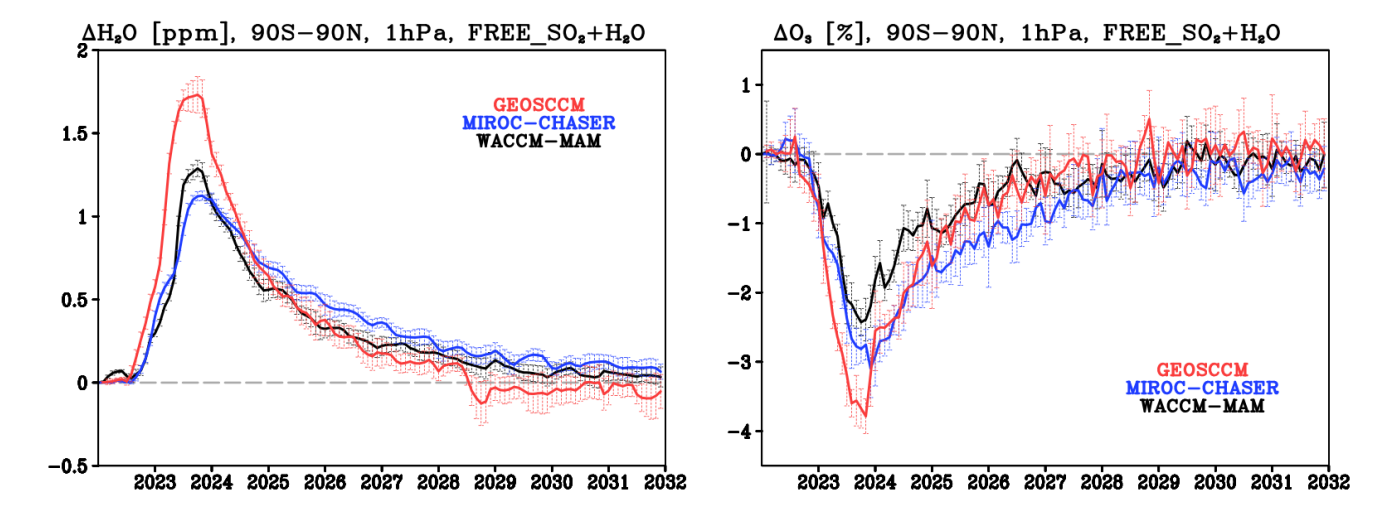


Figure 5. Timeseries of changes (perturbed minus control) in global mean water vapor (left) and ozone (right) at 1 hPa simulated in the free-running experiment with simultaneous injection of SO_2 and H_2O (FREE_ SO_2+H_2O). Error bars indicate ± 2 standard errors in the difference in means.

In the middle and lower stratosphere, while dynamical processes become more important, the chemical impacts of the eruption are still significant. The presence of aerosols decreases active nitrogen levels (NOx, as illustrated by changes in NO₂ – its dominant component – in Fig. 6a-c and Fig. S5) and slows down the rate of NOx-catalyzed chemical ozone loss due to the enhancement of the heterogeneous N₂O₅ hydrolysis on their surfaces. This agrees with the MLS observational results reported by Santee et al. (2023), and previous model results (Wilmouth et al., 2023; Zhang et al., 2024a). The reduction in stratospheric NOx (Fig. S5) and the resulting increase in middle stratospheric ozone (Fig. 3) is stronger in the nudged simulations with SO₂-only injection than in those that include simultaneous injection of both SO₂ and H₂O (Figs. 3 and S5, row 3 vs row 2). This is partly related to the fact that in the absence of H₂O injection the anomalous SAD extends to higher altitudes (Fig. S1, row 3 vs row 2) as aerosols are smaller and less prone to sedimenting out (Aquila et al., in prep./to be submitted). This larger ozone increase in the middle stratosphere under SO₂-only injection offsets the ozone decrease below, leading to less negative and more positive total column ozone responses in the SH mid- and high latitudes as seen in Fig. 2 (row 3 vs row 2).

Another set of heterogeneous reactions on aerosol surfaces involves halogens (chlorine and bromine). This effect leads to a significant enhancement of active chlorine and bromine species ($ClOx = Cl + ClO + 2 \cdot Cl_2O_2 + HOCl + OClO + 2 \cdot Cl_2$; and BrOx = Br + BrO + BrCl + HOBr) in the lower stratosphere (Fig. 6d-i; Figs. S6 and S7) resulting in halogen-catalyzed ozone loss under Hunga forcing. Significant perturbations in chlorine species were also observed in the MLS record (Santee et al., 2023; Wilmouth et al., 2023) and previous model studies (Zhang et al., 2024b). Notably, the simulations show substantial enhancements of BrOx in the lower stratosphere (up to a few ppt, i.e. ~30-80% of the background values, see Fig. S4).



265

270



Unlike the ClOx enhancement, which is largest in absolute terms inside the polar vortex during austral winter and spring, substantial BrOx enhancement occurs throughout the year, thus likely constituting an important chemical contributor to the SH mid-latitude ozone loss (although the ClOx enhancement outside the polar vortex, whilst smaller in absolute terms, still constitutes a relatively large percentage increase, see Fig. S4, and is thus also important). In all three models most of the anomalous halogen repartitioning in the lower stratosphere (Figs. S6 and S7) and the resulting lower stratospheric ozone reduction (Fig. 3) is driven by the aerosol forcing (row 3 in Figs. S6, S7 and 3), with the H₂O forcing in isolation having a relatively small chemical impact (row 4 in Figs. S6, S7 and 3) based on the nudged simulations.

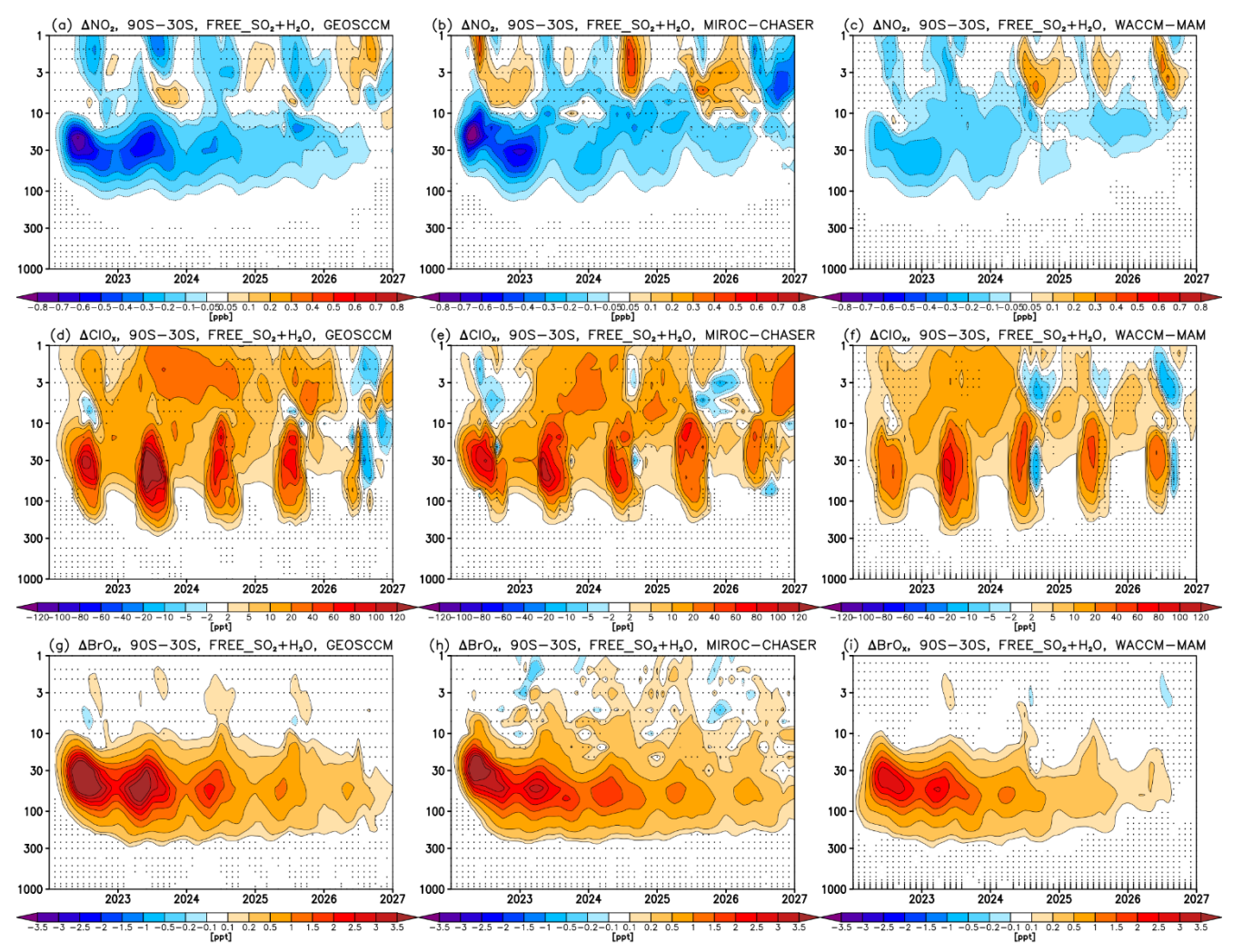


Figure 6. Pressure vs time changes (perturbed minus control) in 90°S-30°S average NO₂ (row 1; a-c), ClOx (row 2; d-f; with ClOx = Cl + ClO + 2·Cl₂O₂ + HOCl + OClO + 2·Cl₂) and BrOx (row 3; g-i; with BrOx = Br + BrO + BrCl + HOBr) simulated in the free-running experiment with simultaneous injection of SO₂ and H₂O (FREE_SO₂+H₂O) in GEOSCCM (left; a,d,g), MIROC-CHASER (middle; b,e,h) and WACCM-MAM (right; c,f,i). Stippling marks regions where the response is not statistically significant (defined as in Fig. 1). See Fig. S4 (supplement) for changes expressed as a percentage relative to the values in the control, and Figs. S5-S7 (supplement) for the changes simulated in the nudged experiments.



285

290

295

300

305



3.3. Changes in dynamical ozone drivers

Aside from direct chemically driven impacts (which are isolated by the nudged Hunga minus control simulations), the freerunning responses also include contributions from the Hunga-induced changes in atmospheric temperatures and transport. Changes in atmospheric temperatures themselves are driven both directly by changes in radiatively active constituents – mainly the anomalous water vapor and aerosols, but also the associated changes in stratospheric ozone itself – and indirectly via the associated dynamical changes, and both include the forced response to the eruption and also contribution from interannual variability.

To varying degrees all three models show indications of SH extra-tropical cooling from the H₂O radiative forcing (Fig. 7a-c), first in the middle stratosphere and then reaching to slightly higher altitudes following the evolution of the anomalous water vapor (Fig. S2). In the lower stratosphere, there is also a weak warming from aerosol absorption and water vapor long-wave heating during the first half of 2022, but later this is offset by the decrease in ozone itself acting to cool the lower stratosphere due to the reduction of its short-wave absorption. Hence, no lower stratospheric warming can be seen after about mid-2022.

Importantly, both the temperature and the ozone changes are strongly modulated by the associated circulation changes. We illustrate the latter in Fig. 7(d-f) using changes in zonal winds averaged over 70°S-30°S; this averaging region was chosen to encompass both the equatorward and the central part of the SH stratospheric jet to capture changes in both its position and its strength. In particular, GEOSCCM and WACCM-MAM, and to some extent MIROC-CHASER, simulate strengthening of the SH stratospheric zonal winds in the second part of 2022 (Fig. 7d-f). This strengthening of the stratospheric jet is associated with a weakening of the large-scale circulation (e.g., Wang et al., 2023) as well as adiabatic cooling and reduction in ozone transport from the tropics and higher altitudes, thereby amplifying the extra-tropical stratospheric cooling (Fig. 7a-c) and lower stratospheric ozone reductions (Fig. 3a-c). These circulation changes also lead to the reduction in stratosphere-to-troposphere ozone transport and tropospheric ozone in Fig. 4. The dominance of the transport effect can be inferred from the significantly smaller tropospheric ozone and O3S anomalies simulated in the nudged simulations, see Fig. S3. Similar strengthening of the SH stratospheric jet is also found in WACCM-MAM in 2023 and in GEOSCCM in 2023, 2024 and 2025 but not in MIROC-CHASER, which helps to explain the varying degrees of persistence of the lower stratospheric ozone reductions across these models seen in Fig. 3a-c.

These circulation anomalies partially reflect the forced response to the Hunga forcing but are also indicative of the large natural interannual variability characterizing the extra-tropical stratosphere. As shown in Bednarz et al. (2025) using the 30-member WACCM-MAM ensemble, the forced dynamical response to the Hunga eruption in both hemispheres is likely



315



relatively weak compared to interannual variability. The role such large interannual variability plays in the diagnosed ozone response to Hunga is illustrated in Fig. 8 (again using the 30-member WACCM-MAM ensemble), exemplified by the Antarctic total column ozone response in September-October-November 2023. While a total column ozone response of ~20 DU was diagnosed from the model based on all 30 members (black solid line), with half of it attributed to chemical changes (black dashed line) and half to dynamical changes based on the comparison with the corresponding nudged simulations, a very large spread of potential ozone responses is found if only a small subset of the ensemble is used for the diagnosis (blue and red lines). This suggests that (i) large model ensembles are needed to confidently diagnose the forced ozone response to the eruption, and (ii) such forced response is unlikely to be detectable in the observational record, which essentially constitutes just one realization.

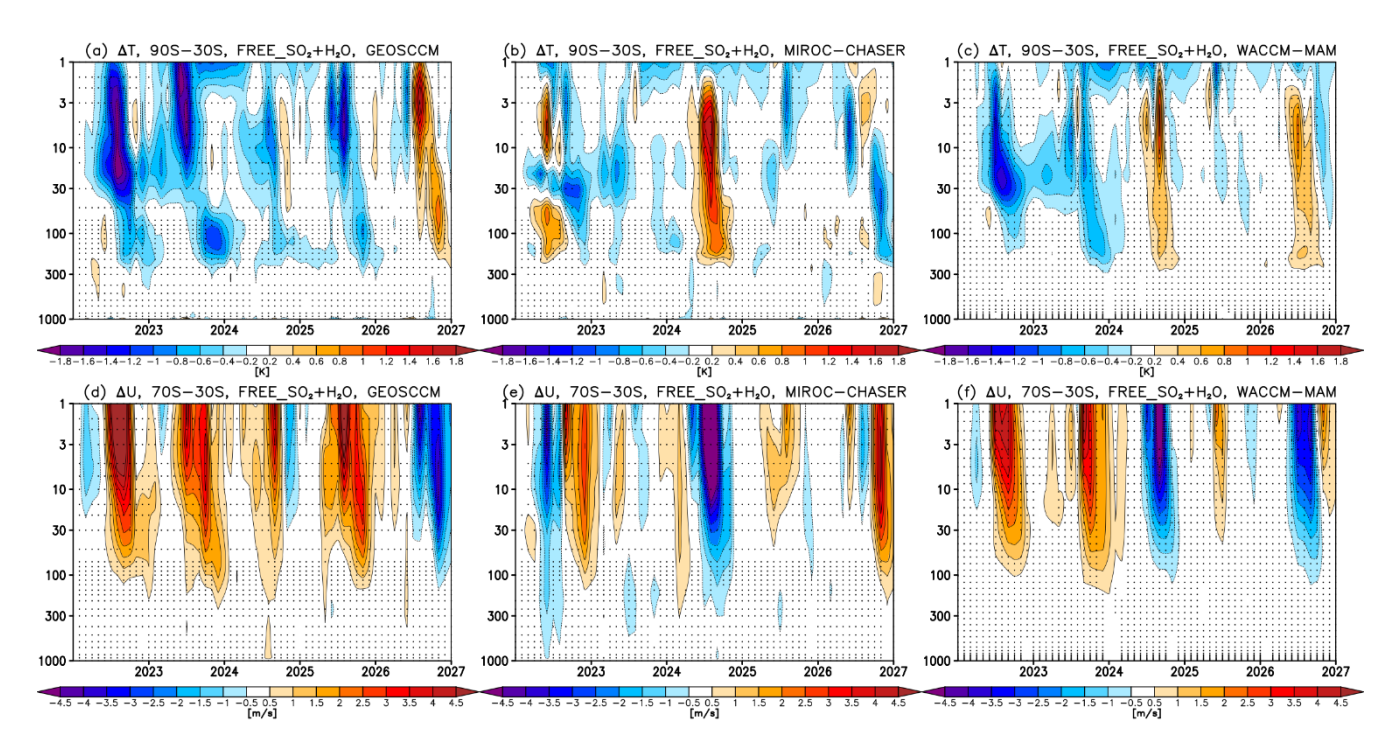


Figure 7. Pressure vs time changes (perturbed minus control) in 90°S-30°S average temperature T (row 1, a-c) and 70°S-30°S average zonal wind U (row 2, d-f) simulated in the free-running experiment with simultaneous injection of SO₂ and H₂O (FREE_SO₂+H₂O) in GEOSCCM (left; a,d), MIROC-CHASER (middle; b,e) and WACCM-MAM (right; c,f). Stippling marks regions where the response is not statistically significant (defined as in Fig. 1).

14



335

340



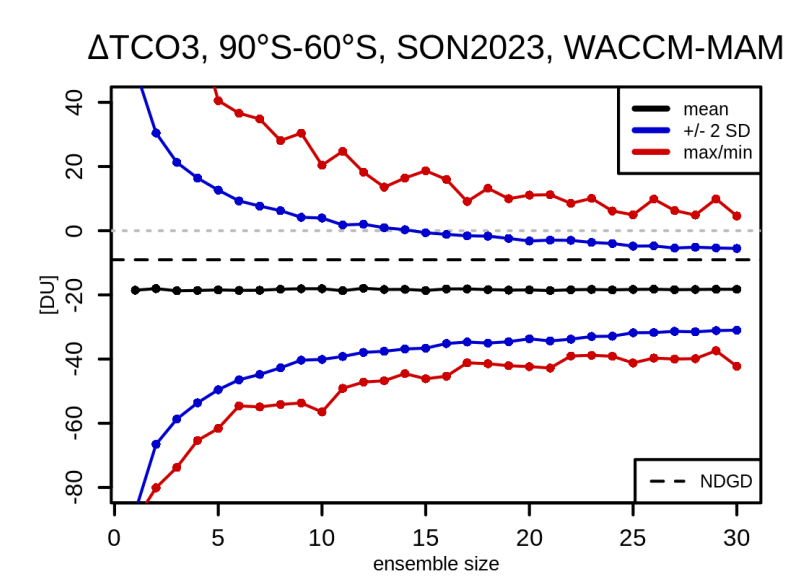


Figure 8. Detectability of the September-October-November (SON) 2023 Antarctic total column ozone (TCO3) response in the free-running simulation with the simultaneous injection of SO2 and H2O in WACCM-MAM. Results obtained by randomly subsampling each ensemble with replacement to obtain 2000 artificial ensembles each of different ensemble size. Black lines denote the mean response, and blue and red lines indicate the ±2 standard deviation and the maximum/minimum ranges, respectively, of the possible responses. The dashed black line denotes the response obtained from the corresponding nudged simulation.

3.4. Radiative impacts on ozone from H₂O injection

An important limitation of inferring the direct chemical response to the Hunga eruption based solely on the perturbed minus control pairs of nudged simulations, as done in Section 3.2, is that such an experimental setup, by design, does not include any chemical changes caused by the significant stratospheric cooling induced by the anomalous water vapor (as the same temperature and wind data are used in the perturbed and control simulations). For that reason, Fig. 9. includes ozone responses simulated by three models that performed free-running simulations with H₂O injection only (CMAM, GSFC2D, and MIROC-CHASER). As expected, all models show an H₂O-induced reduction in ozone in the upper stratosphere. However, all three models show increases in ozone in the middle stratosphere, and CMAM and GSFC2D also show substantial ozone decreases in the lower stratosphere. Notably, such middle stratospheric ozone increases and lower stratospheric decreases were largely absent in the H₂O-only simulations carried out by models in the nudged configuration (Fig. 3, row 4) which, by design, do not include H₂O-induced temperature changes. Furthermore, the nudged H₂O-only experiment in GSFC2D also shows a lack of middle stratospheric ozone increase and a reduced magnitude of the lower stratospheric ozone decrease compared to its free-running counterpart (Fig. 10b,d). These ozone responses in the free-running simulations forced by Hunga water only are thus likely largely indicative of the radiative impact of increased H₂O on concentrations of chemical species of relevance for ozone chemistry, including middle stratospheric NO₂ decrease and



355



lower stratospheric ClOx and BrOx increase (Fig. S9), driven by temperature dependence of their gas phase chemistry and/or temperature dependence of the relevant heterogeneous chemistry, including uptake coefficients and the formation of binary aerosols and PSCs (e.g. Carslaw et al., 1997; Solomon et al., 2015).

Finally, while the changes in chemical tracers described above could also be caused by a dynamical response to the H₂O-induced cooling (Fig. S8), the GSFC2D model, by design, does not simulate any internal dynamical response and as such changes in circulation in this model are minimal and due only to the small direct response to the Hunga radiative forcing (Fig. S8, middle). In addition, both Wang et al. (2023) and Yook et al. (2025) showed that the use of H₂O-only forcing is insufficient to capture the Hunga dynamical response, and that simultaneous injection of both SO₂ and H₂O is needed to obtain a SH dynamical response resembling that found in reanalyses. Nonetheless, we note that dynamics do play a role in CMAM, which shows a significant strengthening of zonal winds in late 2022 (Fig. S8, left); this amplifies the stratospheric cooling and also reduces ozone transport, thus contributing to the lower stratospheric ozone decrease seen in the model in late 2022 (Fig. 9).

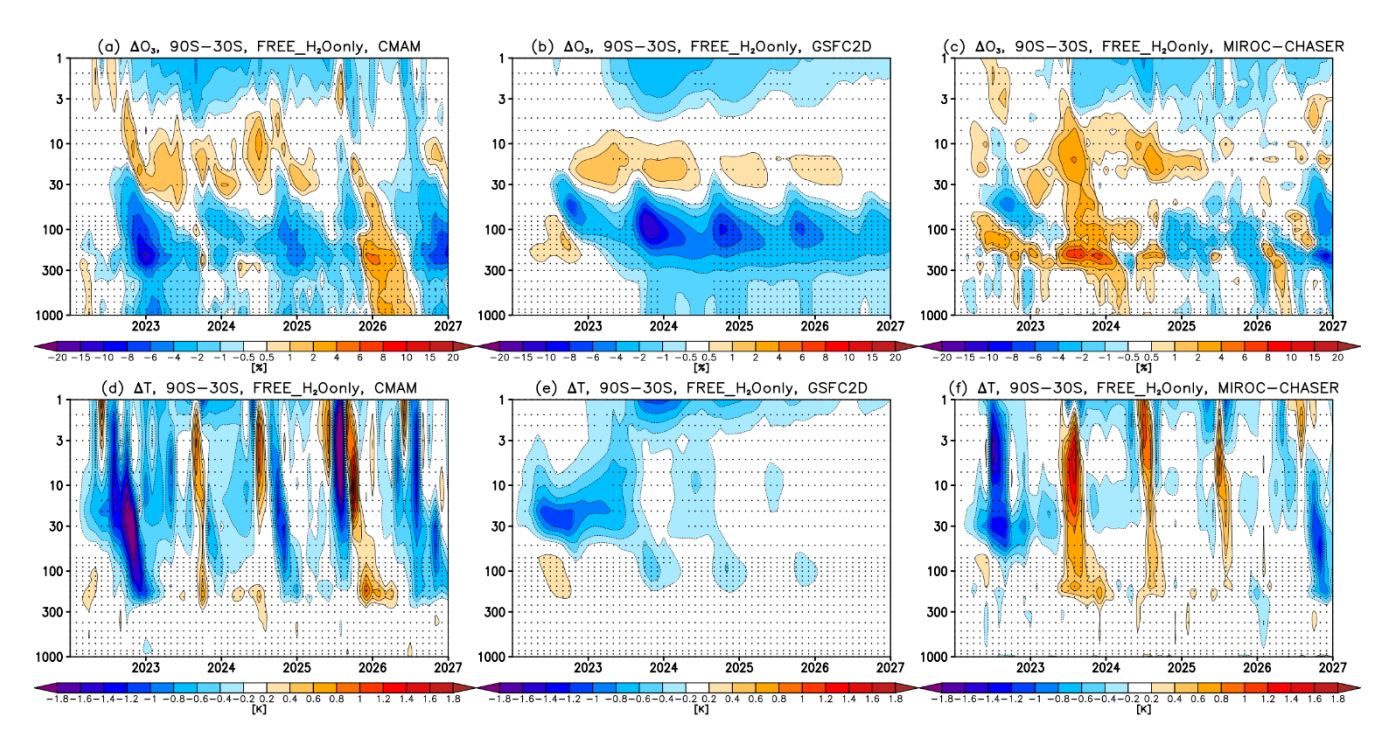


Figure 9. Pressure vs time changes (perturbed minus control) in 90°S-30°S average ozone (row 1; a-c) and temperature (row 2; d-f) simulated in the free-running experiment with H2O-only injection (FREE_H2Oonly) in CMAM (left; a,d), GSFC2D (middle; b,e) and MIROC-CHASER (right; c,f). Stippling marks regions where the response is not statistically significant (defined as in Fig. 1).





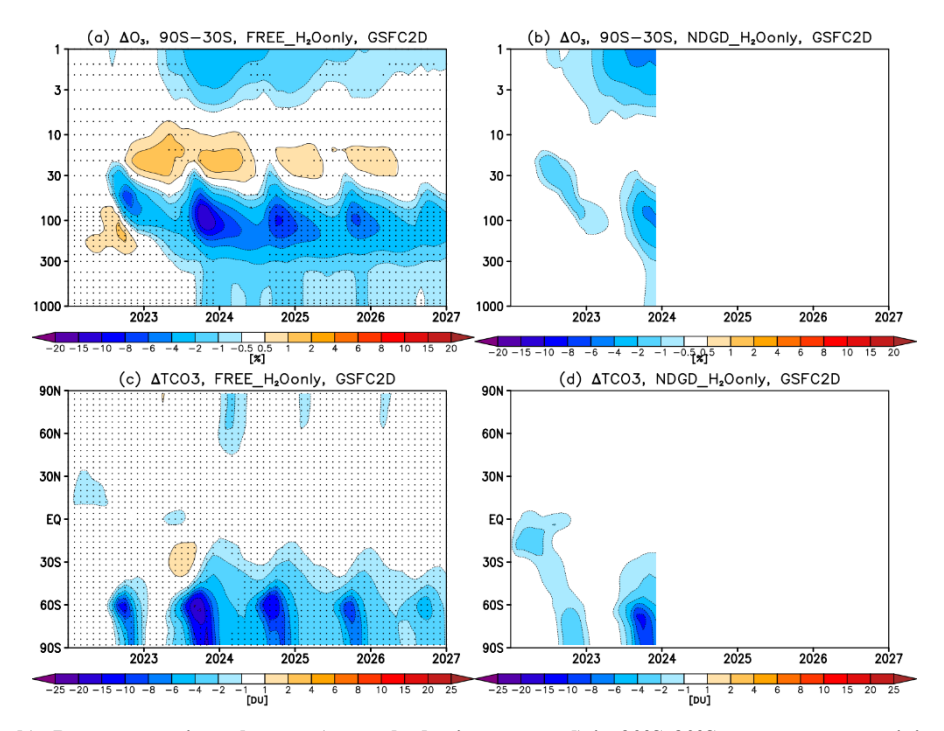


Figure 10. Row 1 (a-b): Pressure vs time changes (perturbed minus control) in 90°S-30°S average ozone mixing ratios simulated in GSFC2D with H2O-only injection in the free-running experiment (FREE_H2Oonly; left) and in the nudged experiment (NDGD_H2Oonly; right). Row 2 (c-d): the corresponding latitude vs time changes in total column ozone. Stippling in left column marks regions where the response is not statistically significant (defined as in Fig. 1).

4. Summary and discussion

375

380

This study assessed the impact of the 2022 Hunga eruption on stratospheric ozone using a multi-model ensemble of chemistry-climate model simulations. The models simulated the impacts of both water vapor and aerosol perturbations from Hunga, either together or separately, and were run using free-running and specified dynamics ('nudged') configurations, allowing for a detailed assessment of not just ozone impacts but also the relative importance of changes in different chemical and dynamical drivers.

All three models for which free-running experiments with simultaneous injection of SO₂ and H₂O were carried out simulated ozone decreases in the SH mid- and high latitudes, confirming the role of the eruption in contributing to the anomalously low SH mid-latitude ozone abundances observed by satellite instruments in 2022. However, the models differed with respect to both the strength and the persistence of the ozone changes, in particular for polar ozone, with Antarctic ozone reductions in late 2023 ranging from statistically not significant losses of less than 10 DU in MIROC-CHASER to significant ozone losses of up to 50 DU in GEOSCCM. Our simulations suggest that Hunga impacts on ozone are not just limited to the stratosphere



385

410

415



(and above), with smaller SH extra-tropical ozone losses of a few percent extending into the troposphere and to the surface as the result of reduced stratosphere-to-troposphere ozone transport.

Our results suggest that the Hunga-induced chemical impact was as important as the dynamical impact in determining the overall SH extra-tropical ozone response to the eruption. The simulations show modest chemical ozone changes driven by anomalous chemical processing on aerosol surfaces and water-induced stratospheric cooling, including chlorine, bromine and nitrogen repartitioning. These changes manifest as ozone decreases in the lower stratosphere and ozone increases in the middle stratosphere. These chemical changes occur alongside dynamical contributions from altered circulation and ozone 390 transport. In comparison, previous studies looking at the origins of the ozone anomalies found in the observational record concluded that dynamical changes were the primary driver of exceptional ozone reductions observed in the SH mid-latitudes in 2022 (Santee et al., 2023; Zhang et al., 2024a; Wilmouth et al., 2023), but the extent to which this anomalous dynamical variability was a forced response to the eruption as opposed to a manifestation of the very large interannual variability characterizing the extra-tropical stratosphere was not clear. Our model simulations were designed to isolate the forced 395 response to the eruption, and they suggest that chemical and dynamical changes are comparable in importance in determining the overall Hunga ozone response. Our study further illustrates that the forced response to Hunga is much weaker than the natural interannual variability, hindering confident detection of the Hunga response from small model ensembles or a relatively short observational record (which effectively constitutes just one realization).

400 Regarding the chemical impacts in the lower stratosphere, the model simulations indicate that the Hunga SO₂ injection, rather than the H₂O injection, is likely the primary chemical driver of the SH extra-tropical ozone change, with aerosolinduced changes in the efficiency of the chlorine, bromine and nitrogen catalytic loss cycles all contributing to the Hunga ozone response. The importance of bromine in influencing atmospheric chemistry following volcanic eruptions was pointed out before by Berthet et al. (2017), but in general is difficult to confirm in observations since the low atmospheric 405 concentrations of many bromine species hinder their detection.

Finally, while our results suggest that while Hunga may continue to exert a small influence on ozone until ~2027-2028 as the anomalous water vapor and aerosol are gradually removed from the atmosphere, the contribution of natural dynamical variability will likely hinder the detection of such weak perturbations on ozone. As such, the most robust Hunga ozone signal is expected in the upper stratosphere (and above in the lower mesosphere) due to the dominance of photochemical processes in driving ozone abundances in that region, where models suggest a small (up to ~2-4%) Hunga water-driven ozone reduction persisting at reduced magnitude until around 2028. Notably, the fidelity of the mode-simulated Hunga impacts, in particular in the near future, will partially depend on the rate at which Hunga water and aerosols are removed from the atmosphere, which in turn is related to the models' skill in reproducing the observed evolution of the Hunga water and aerosol enhancements (this issue of model skill is analysed in depth by Zhuo et al. (2025) and Aquila et al. (in prep/to be





submitted)). All in all, our study confirms the eruption's role in modulating stratospheric ozone abundances in the short term, but also highlights the associated uncertainties and the presence of large natural variability, all of which makes confident attribution of Hunga impacts an ongoing challenge.

Acknowledgements:

- EMB acknowledges support by the National Oceanic and Atmospheric Administration (NOAA) cooperative agreement NA22OAR4320151, NOAA Earth Radiative Budget (ERB) program, and Reflective fellowship program. F.F.Ø. acknowledges support from the European Commission Horizon 2020 research and innovation program under the Marie Skłodowska-Curie grant no. 891186. Work at the Jet Propulsion Laboratory, California Institute of Technology, was carried out under a contract with the National Aeronautics and Space Administration (80NM0018D0004).
- This work used JASMIN, the UK's collaborative data analysis environment (https://www.jasmin.ac.uk). We would also like to acknowledge high-performance computing support from Derecho and Casper, provided by the National Center for Atmospheric Research (NCAR) Computational and Information Systems Laboratory, sponsored by the National Science Foundation.

430 Conflict of Interest

EMB and ST are members of the editorial board of ACP.

References:

- Aquila, V., R. Ueyama, A. Bourassa, S. Khaykin, E. Asher, A. Baron, E. M. Bednarz, S. Bekki, C. Brühl, P. Case, S. Chabrillat, M. Clyne, P. Colarco, D. Cugnet, S. Dhomse, L. Falletti, N. Lebas, C.-C. Liu, G. Mann, M. Marchand, P. Newman, Y. Peng, I. Quaglia, S. Remy, L. Rieger, A. Rozanov, M. Schoeberl, T. Sekiya, G. L. Stenchikov, S. Tilmes, S. Watanabe, X. Wang, P. Yu, W. Yu, J. Zhang, Y. Zhu, Zh. Zhuo: "Modeling the medium-term evolution of aerosols and water vapor from the Hunga eruption", 2025 (in prep./to be submitted).
- E. Asher, M. Todt, K. Rosenlof, T. Thornberry, R. Gao, G. Taha, P. Walter, S. Alvarez, J. Flynn, S.M. Davis, S. Evan, J. Brioude, J. Metzger, D.F. Hurst, E. Hall, & K. Xiong: Unexpectedly rapid aerosol formation in the Hunga Tonga plume, *Proc. Natl. Acad. Sci. U.S.A.* 120 (46) e2219547120, https://doi.org/10.1073/pnas.2219547120, 2023.



450



- Banerjee, A., Maycock, A. C., Archibald, A. T., Abraham, N. L., Telford, P., Braesicke, P., and Pyle, J. A.: Drivers of changes in stratospheric and tropospheric ozone between year 2000 and 2100, *Atmos. Chem. Phys.*, 16, 2727–2746, https://doi.org/10.5194/acp-16-2727-2016, 2016.
 - Bednarz, E. M., Butler, A. H., Wang, X., Zhuo, Z., Yu, W., Stenchikov, G., Toohey, M., and Zhu, Y.: Indirect climate impacts of the Hunga eruption, EGUsphere [preprint], https://doi.org/10.5194/egusphere-2025-1970, 2025.
- Berthet, G., Jégou, F., Catoire, V., Krysztofiak, G., Renard, J.-B., Bourassa, A. E., Degenstein, D. A., Brogniez, C., Dorf, M., Kreycy, S., Pfeilsticker, K., Werner, B., Lefèvre, F., Roberts, T. J., Lurton, T., Vignelles, D., Bègue, N., Bourgeois, Q., Daugeron, D., Chartier, M., Robert, C., Gaubicher, B., and Guimbaud, C.: Impact of a moderate volcanic eruption on chemistry in the lower stratosphere: balloon-borne observations and model calculations, Atmos. Chem. Phys., 17, 2229–2253, https://doi.org/10.5194/acp-17-2229-2017, 2017.
 - Carslaw, K. S., T. Peter, and S. L. Clegg: Modeling the composition of liquid stratospheric aerosols, *Rev. Geophys.*, 35(2), 125–154, doi:10.1029/97RG00078, 1997.
- 460 Carn, S., Krotkov, N., Fisher, B., and Li, C.: Out of the blue: Volcanic SO2 emissions during the 2021–2022 eruptions of Hunga Tonga—Hunga Ha'apai (Tonga)., *Frontiers in Earth Science* 10: 976962, 2022.
- Carr, J. L., Horváth, Á., Wu, D. L., & Friberg, M. D.: Stereo plume height and motion retrievals for the record-setting Hunga Tonga-Hunga Ha'apai eruption of 15 January 2022, *Geophysical Research Letters*, 49, e2022GL098131, https://doi.org/10.1029/2022GL098131, 2022.
 - Coy, L., Newman, P. A., Wargan, K., Partyka, G., Strahan, S. E., & Pawson, S.: Stratospheric circulation changes associated with the Hunga Tonga-Hunga Ha'apai eruption. *Geophysical Research Letters*, 49, e2022GL100982. https://doi.org/10.1029/2022GL100982, 2022.
- Fleming, E. L., Newman, P. A., Liang, Q., & Oman, L. D.: Stratospheric temperature and ozone impacts of the Hunga Tonga-Hunga Ha'apai water vapor injection. *Journal of Geophysical Research: Atmospheres*, 129, e2023JD039298. https://doi.org/10.1029/2023JD039298, 2024.
- Gelaro, R., McCarty, W., Suárez, M. J., Todling, R., Molod, A., Takacs, L., Randles, C. A., Darmenov, A., Bosilovich, M. G., Reichle, R., Wargan, K., Coy, L., Cullather, R., Draper, C., Akella, S., Buchard, V., Conaty, A., da Silva, A. M., Gu, W., Kim, G., Koster, R., Lucchesi, R., Merkova, D., Nielsen, J. E., Partyka, G., Pawson, S., Putman, W., Rienecker, M.,



480



Schubert, S. D., Sienkiewicz, M., and Zhao, B.: The Modern-Era Retrospective Analysis for Research and Applications, Version 2 (MERRA-2), *J. Climate*, 30, 5419–5454, https://doi.org/10.1175/JCLI-D-16-0758.1, 2017.

Gettelman, A., Mills, M. J., Kinnison, D. E., Garcia, R. R., Smith, A. K., Marsh, D. R., Tilmes, S., Vitt, F., Bardeen, C. G., McInerny, J., Liu, H.-L., Solomon, S. C., Polvani, L. M., Emmons, L. K., Lamarque, J.-F., Richter, J. H., Glanville, A. S., Bacmeister, J. T., Phillips, A. S., Neale, R. B., Simpson, I. R., DuVivier, A. K., Hodzic, A., and Randel, W. J.: The Whole Atmosphere Community Climate Model Version 6 (WACCM6), *J. Geophys. Res.-Atmos.*, 124, 12380–12403, https://doi.org/10.1029/2019JD030943, 2019.

Khaykin, S., Podglajen, A., Ploeger, F., Grooß, J.-U., Tence, F., Bekki, S., Khlopenkov, K., Bedka, K., Rieger, L., Baron, A., Godin-Beekmann, S., Legras, B., Sellitto, P., Sakai, T., Barnes, J., Uchino, O., Morino, I., Nagai, T., Wing, R., Baumgarten, G., Gerding, M., Duflot, V., Payen, G., Jumelet, J., Querel, R., Liley, B., Bourassa, A., Clouser, B., Feofilov, A.,
Hauchecorne, A., and Ravetta, F.: Global perturbation of stratospheric water and aerosol burden by Hunga eruption, Commun. Earth Environ., 3, 316, https://doi.org/10.1038/s43247-022-00652-x, 2022.

Manney, G. L., Santee, M. L., Lambert, A., Millán, L. F., Minschwaner, K., Werner, F., Lawrence, Z. D., Read, W. G., Livesey, N. J., Wang, T.: Siege in the southern stratosphere: Hunga Tonga-Hunga Ha'apai water vapor excluded from the
2022 Antarctic polar vortex. *Geophysical Research Letters*, 50, e2023GL103855, https://doi.org/10.1029/2023GL103855, 2023.

Millán, L., Santee, M. L., Lambert, A., Livesey, N. J., Werner, F., Schwartz, M. J., Pumphrey, H. C., Manney, G. L., Wang, Y., Su, H., Wu, L., Read, W. G., and Froidevaux, L.: The Hunga Tonga-Hunga Ha'apai Hydration of the Stratosphere,
Geophys. Res. Lett., 49, e2022GL099381, https://doi.org/10.1029/2022GL099381, 2022.

Molod, A., Takacs, L., Suarez, M., and Bacmeister, J.: Development of the GEOS-5 atmospheric general circulation model: evolution from MERRA to MERRA2, *Geosci. Model Dev.*, 8, 1339–1356, https://doi.org/10.5194/gmd-8-1339-2015, 2015. Proud, Simon R., Andrew T. Prata, and Simeon Schmauß. "The January 2022 eruption of Hunga Tonga-Hunga Ha'apai volcano reached the mesosphere." *Science* 378.6619: 554-557, 2022.

Randel, W. J., Wang, X., Starr, J., Garcia, R. R., & Kinnison, D.: Long-term temperature impacts of the Hunga volcanic eruption in the stratosphere and above. *Geophysical Research Letters*, 51, e2024GL111500. https://doi.org/10.1029/2024GL111500, 2024



530



Reinecker, M., Suarez, M., Todling, R., Bacmeister, J., Takacs, L., & Liu, H.: The GEOS-5 data assimilation system-documentation of versions 5.0. 1, 5.1. 0 (No. NASA Tech Rep TM-2007, 104606), 2008.

- Santee, M.L., A. Lambert, L. Froidevaux, G.L. Manney, M.J. Schwartz, L.F. Millán, N.J. Livesey, W.G. Read, F. Werner, and R.A. Fuller: Strong evidence of heterogeneous processing on stratospheric sulfate aerosol in the extrapolar Southern Hemisphere following the 2022 Hunga Tonga-Hunga Ha'apai eruption. *Journal of Geophysical Research: Atmospheres*, 128, e2023JD039169, doi: 10.1029/2023JD039169, 2023.
- Santee, M.L., G. L. Manney, A. Lambert, L.F. Millán, N.J. Livesey, M.C. Pitts, L. Froidevaux, W.G. Read, and R.A. Fuller:

 The influence of stratospheric hydration from the Hunga eruption on chemical processing in the 2023 Antarctic vortex. *Journal of Geophysical Research: Atmospheres*, 129, e2023JD040687, doi: 10.1029/2023JD040687, 2024.
- Scinocca, J. F., McFarlane, N. A., Lazare, M, Li, J., and Plummer, D.: Technical Note: The CCCma third generation AGCM and its extension into the middle atmosphere, *Atmos. Chem. Phys.*, 8, 7055–7074, https://doi.org/10.5194/acp-8-7055-2008, 2008.
 - Schoeberl, M. R., Wang, Y., Taha, G., Zawada, D. J., Ueyama, R., & Dessler, A.:. Evolution of the climate forcing during the two years after the Hunga Tonga-Hunga Ha'apai eruption. *Journal of Geophysical Research: Atmospheres*, 129, e2024JD041296. https://doi.org/10.1029/2024JD041296, 2024.
 - Schoeberl, M. R., Wang, Y., Ueyama, R., Dessler, A., Taha, G., & Yu, W.: The estimated climate impact of the Hunga Tonga-Hunga Ha'apai eruption plume: *Geophysical Research Letters*, 50, e2023GL104634, https://doi.org/10.1029/2023GL104634, 2023.
- 535 Sekiya, T., K. Sudo, and T. Nagai: Evolution of stratospheric sulfate aerosol from the 1991 Pinatubo eruption: Roles of aerosol microphysical processes, *J. Geophys. Res. Atmos.*, 121, 2911–2938, doi:10.1002/2015JD024313, 2016.
- Sellitto, P., Siddans, R., Belhadji, R., Carboni, E., Legras, B., Podglajen, A., et al.: Observing the SO2 and sulfate aerosol plumes from the 2022 Hunga eruption with the Infrared Atmospheric Sounding Interferometer (IASI). *Geophysical Research* Letters, 51, e2023GL105565, 2024.
 - Solomon, S., D. Kinnison, J. Bandoro, and R. Garcia: Simulation of polar ozone depletion: An update. *J. Geophys. Res. Atmos.*, 120, 7958–7974. doi: 10.1002/2015JD023365, 2015.



555



- Stenchikov, G., Ukhov, A., & Osipov, S.: Modeling the radiative forcing and atmospheric temperature perturbations caused by the 2022 Hunga volcano explosion. *Journal of Geophysical Research: Atmospheres*, 130, e2024JD041940. https://doi.org/10.1029/2024JD041940, 2025.
- Stocker, M., Steiner, A.K., Ladstädter, F. et al: Strong persistent cooling of the stratosphere after the Hunga eruption. 550 *Commun Earth Environ* 5, 450 (2024). https://doi.org/10.1038/s43247-024-01620-3, 2024.
 - Yook, S., Solomon, S., & Wang, X.: The Impact of 2022 Hunga Tonga-Hunga Ha'apai (Hunga) Eruption on Stratospheric Circulation and Climate, *Journal of Geophysical Research: Atmospheres*, 130, e2024JD042943. https://doi.org/10.1029/2024JD042943, 2025.
 - Vömel, H. Evan, S., Tully, M.:Water vapor injection into the stratosphere by Hunga Tonga-Hunga Ha'apai, *Science*, 377,1444-1447, DOI:10.1126/science.abq2299, 2022.
- Wang, X., Randel, W., Zhu, Y., Tilmes, S., Starr, J., Yu, W., et al.: Stratospheric climate anomalies and ozone loss caused by the Hunga Tonga-Hunga Ha'apai volcanic eruption. *Journal of Geophysical Research: Atmospheres*, 128(22), e2023JD039480. https://doi.org/10.1029/2023JD039480, 2023.
- D.M. Wilmouth, F.F. Østerstrøm, J.B. Smith, J.G. Anderson, & R.J. Salawitch: Impact of the Hunga Tonga volcanic eruption on stratospheric composition, *Proc. Natl. Acad. Sci. U.S.A.* 120 (46) e2301994120, https://doi.org/10.1073/pnas.2301994120, 2023.
 - Wohltmann, I., Santee, M. L., Manney, G. L., & Millán, L. F.: The chemical effect of increased water vapor from the Hunga Tonga-Hunga Ha'apai eruption on the Antarctic ozone hole. *Geophysical Research Letters*, 51, e2023GL106980. https://doi.org/10.1029/2023GL106980, 2024.
 - Zhang, J., Kinnison, D., Zhu, Y., Wang, X., Tilmes, S., Dube, K., & Randel, W.: Chemistry contribution to stratospheric ozone depletion after the unprecedented water-rich Hunga Tonga eruption. *Geophysical Research Letters*, 51, e2023GL105762. https://doi.org/10.1029/2023GL105762, 2024a.
- Zhang, J., Wang, P., Kinnison, D., Solomon, S., Guan, J., Stone, K., & Zhu, Y.: Stratospheric chlorine processing after the unprecedented Hunga Tonga eruption. *Geophysical Research Letters*, 51, e2024GL108649. https://doi.org/10.1029/2024GL108649, 2024b.





Zhu, Y., Akiyoshi, H., Aquila, V., Asher, E., Bednarz, E. M., Bekki, S., Brühl, C., Butler, A. H., Case, P., Chabrillat, S.,
Chiodo, G., Clyne, M., Colarco, P. R., Dhomse, S., Falletti, L., Fleming, E., Johnson, B., Jörimann, A., Kovilakam, M., Koren, G., Kuchar, A., Lebas, N., Liang, Q., Liu, C.-C., Mann, G., Manyin, M., Marchand, M., Morgenstern, O., Newman, P., Oman, L. D., Østerstrøm, F. F., Peng, Y., Plummer, D., Quaglia, I., Randel, W., Rémy, S., Sekiya, T., Steenrod, S., Sukhodolov, T., Tilmes, S., Tsigaridis, K., Ueyama, R., Visioni, D., Wang, X., Watanabe, S., Yamashita, Y., Yu, P., Yu, W., Zhang, J., and Zhuo, Z.: Hunga Tonga–Hunga Ha'apai Volcano Impact Model Observation Comparison (HTHH-MOC)
project: experiment protocol and model descriptions, *Geosci. Model Dev.*, 18, 5487–5512, https://doi.org/10.5194/gmd-18-5487-2025, 2025.

Zhou, X., S.S. Dhomse, W. Feng, G. Mann, S. Heddell, H. Pumphrey, B.J. Kerridge, B. Latter, R. Siddans, L. Ventress, R. Querel, P. Smale, E. Asher, E.G. Hall, S. Bekki and M.P. Chipperfield: Antarctic vortex dehydration in 2023 as a substantial removal pathway for Hunga Tonga-Hunga Ha'apai water vapour, *Geophysical Research Letters*, **51**, e2023GL107630, doi: 10.1029/2023GL107630, 2024.

Zhuo, Z., Wang, X., Zhu, Y., Bednarz, E. M., Fleming, E., Colarco, P. R., Watanabe, S., Plummer, D., Stenchikov, G., Randel, W., Bourassa, A., Aquila, V., Sekiya, T., Schoeberl, M. R., Tilmes, S., Yu, W., Zhang, J., Kushner, P. J., and Pausata, F. S. R.: Comparing Multi-Model Ensemble Simulations with Observations and Decadal Projections of Upper Atmospheric Variations Following the Hunga Eruption, EGUsphere [preprint], https://doi.org/10.5194/egusphere-2025-665 1505, 2025.